

Supplementary Information

Direct Conversion of Solid g-C₃N₄ into Metal-ended N-doped Carbon Nanotubes for Rechargeable Zn-Air Batteries

Zixuan Zhang^{‡,a}, Yin Wang^{‡,a*}, Jingqi Guan^b, Tingting Zhang^a, Peihe Li^a,

Yin Hao^a, Limei Duan^{a*}, Zhiqiang Niu^c, Jinghai Liu^{a*}

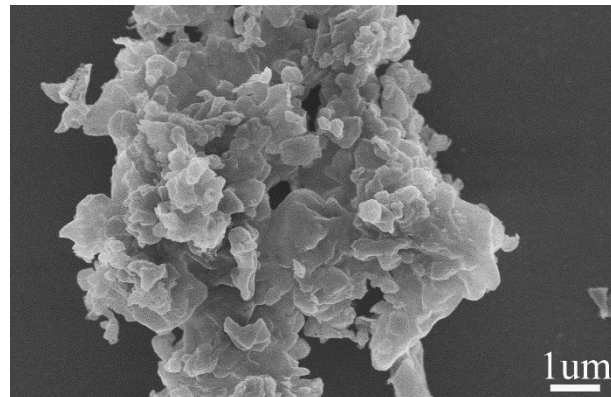


Figure S1. SEM image of g-C₃N₄.

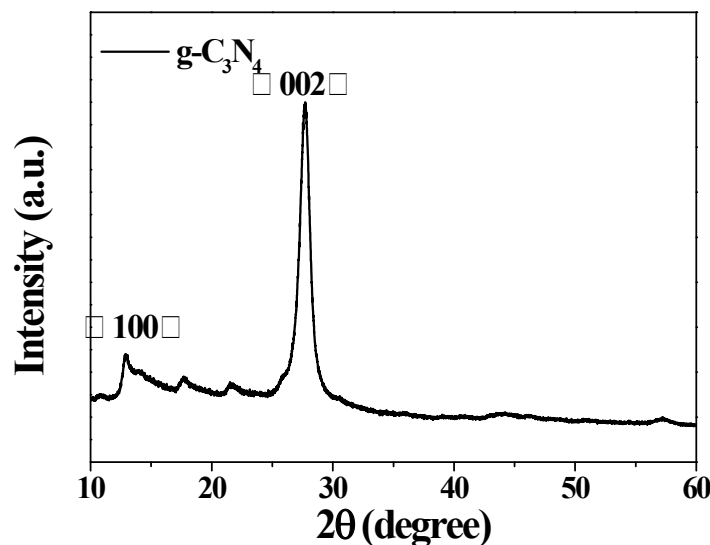


Figure S2. XRD pattern of g-C₃N₄.

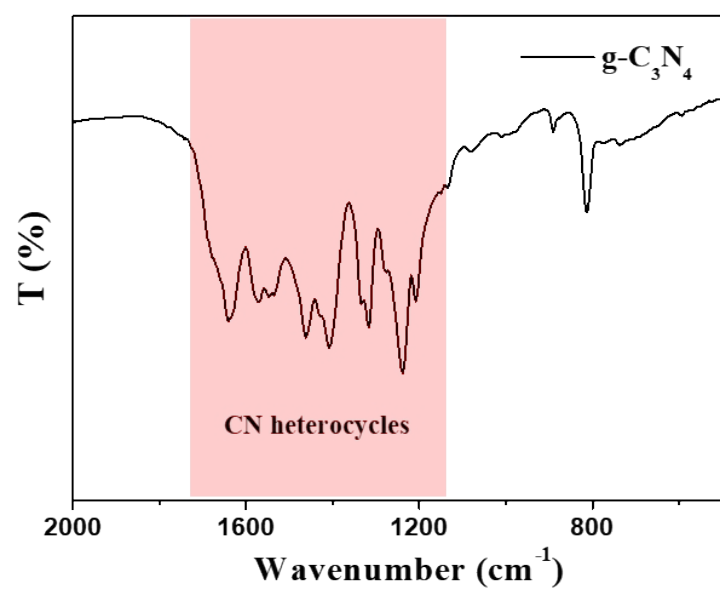


Figure S3. FTIR spectrum of $\text{g-C}_3\text{N}_4$.

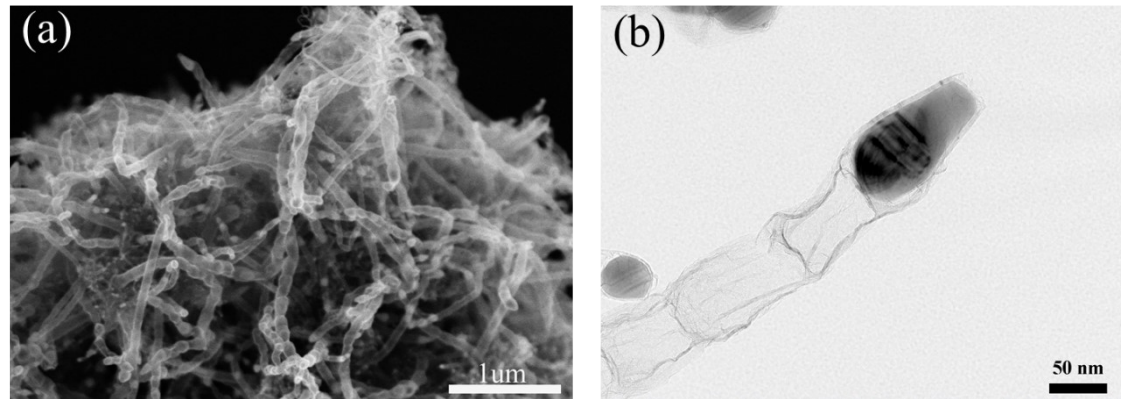


Figure S4. Morphology of Co-NCNTs. (a) SEM image and (b) TEM image.

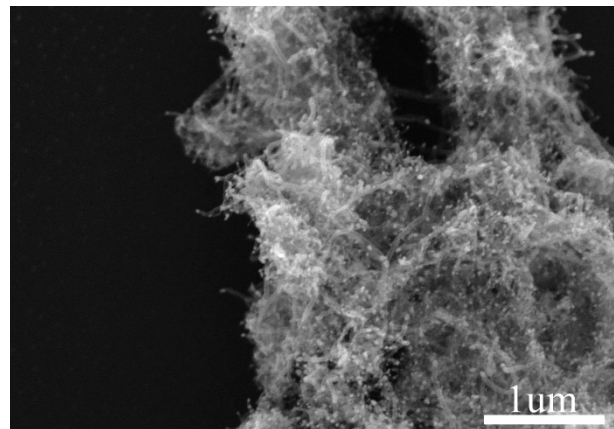


Figure S5. SEM image of Co-NCNTs-2.

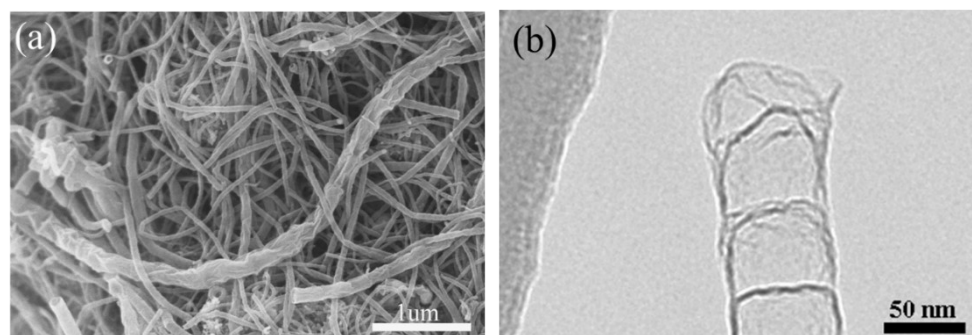


Figure S6. Morphology of Co-NCNTs-N. (a) SEM image and (b) TEM image.

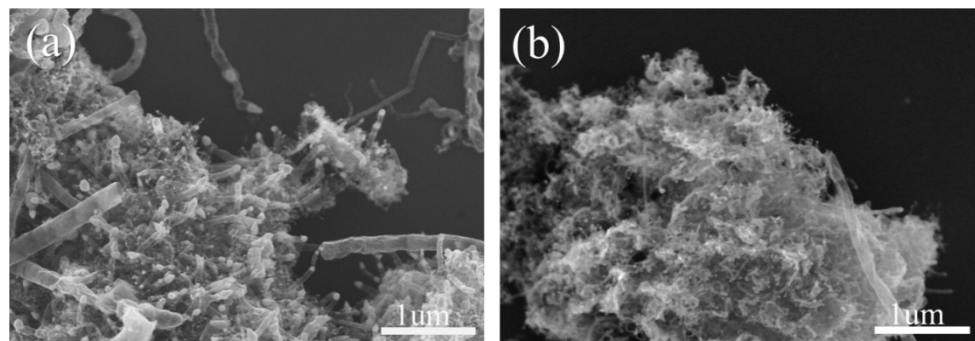


Figure S7. SEM images of (a) Co-NCNTs-S and (b) Co-NCNTs-Cl.

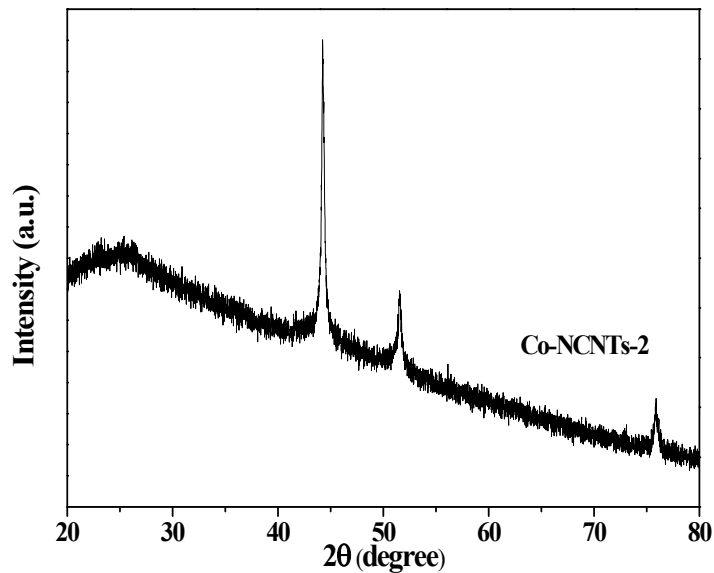


Figure S8. XRD pattern of Co-NCNTs-2.

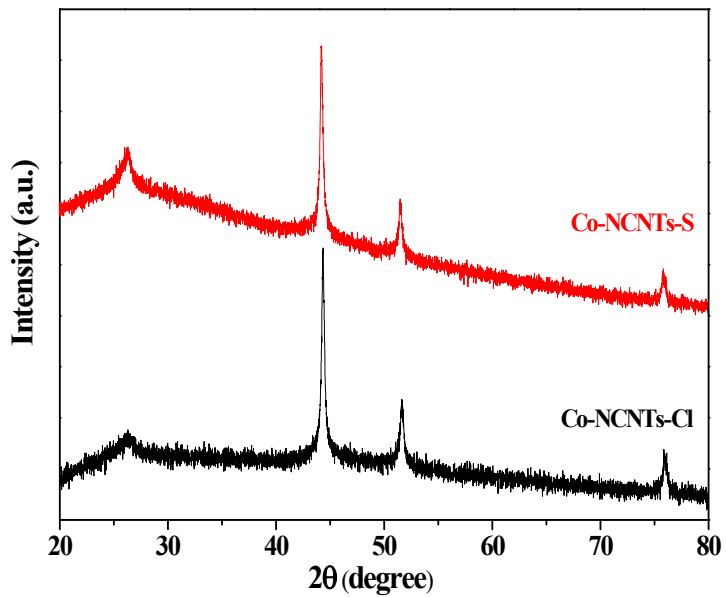


Figure S9. XRD patterns of Co-NCNTs-S and Co-NCNTs-Cl.

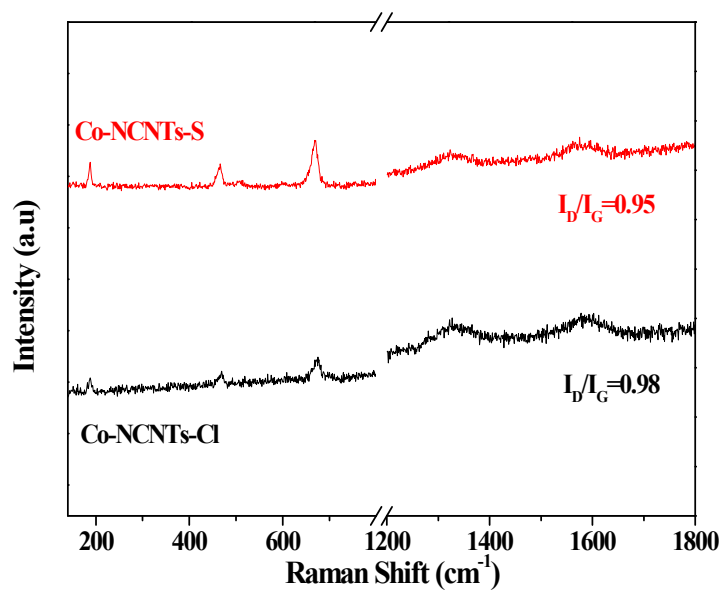


Figure S10. Raman spectra of Co-NCNTs-S and Co-CNTs-Cl.

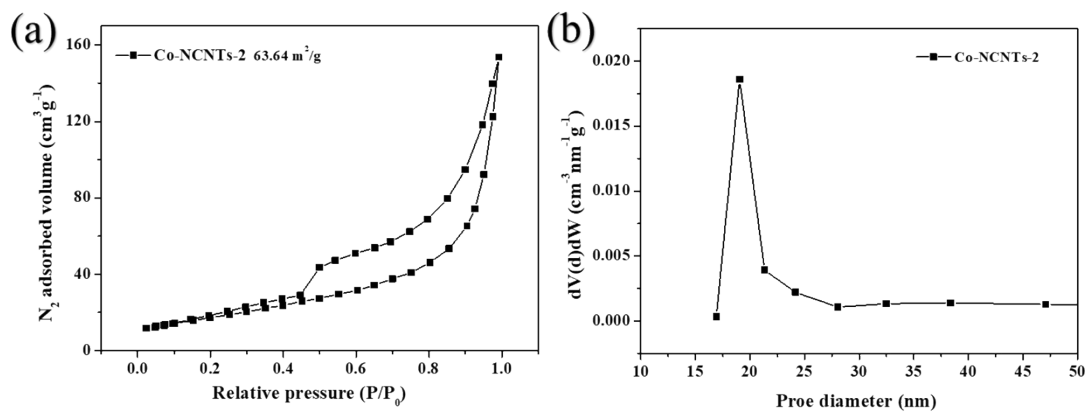


Figure S11. (a) N_2 adsorption/desorption isotherm and (b) pore sizes distributions of Co-NCNTs-2 according to BJH model.

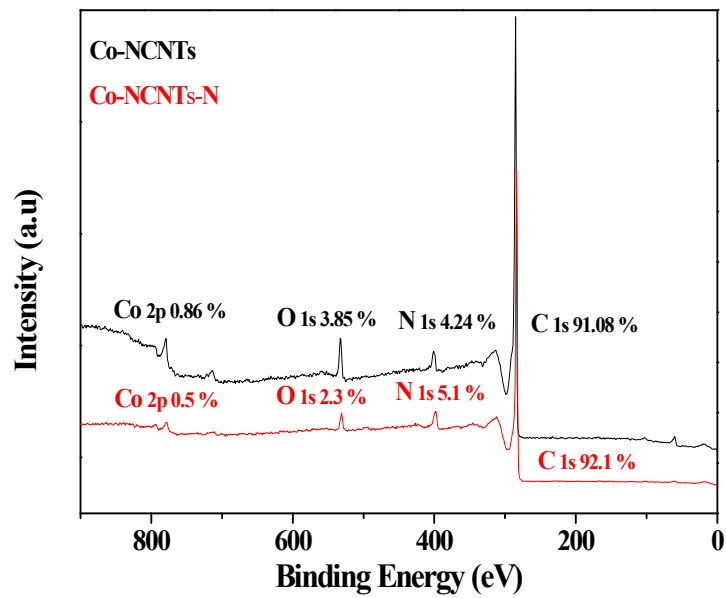


Figure S12. XPS survey spectra of Co-NCNTs and Co-NCNTs-N.

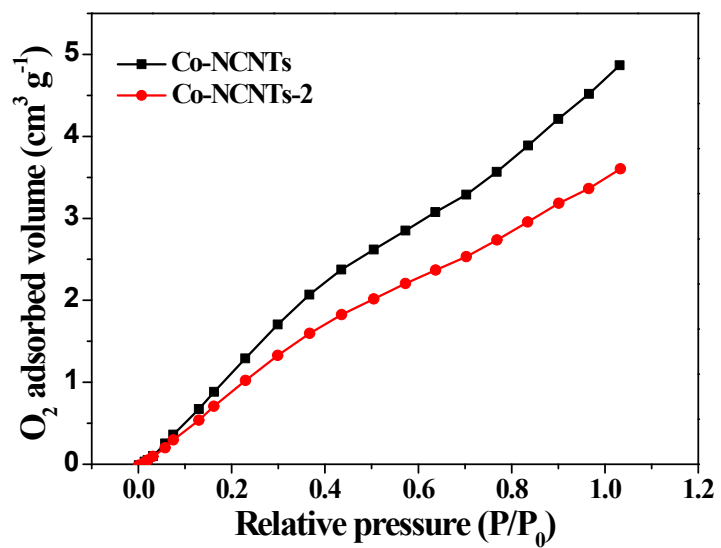


Figure S13. O₂ adsorption isotherms of Co-NCNTs and Co-NCNTs-2 at 25 °C.

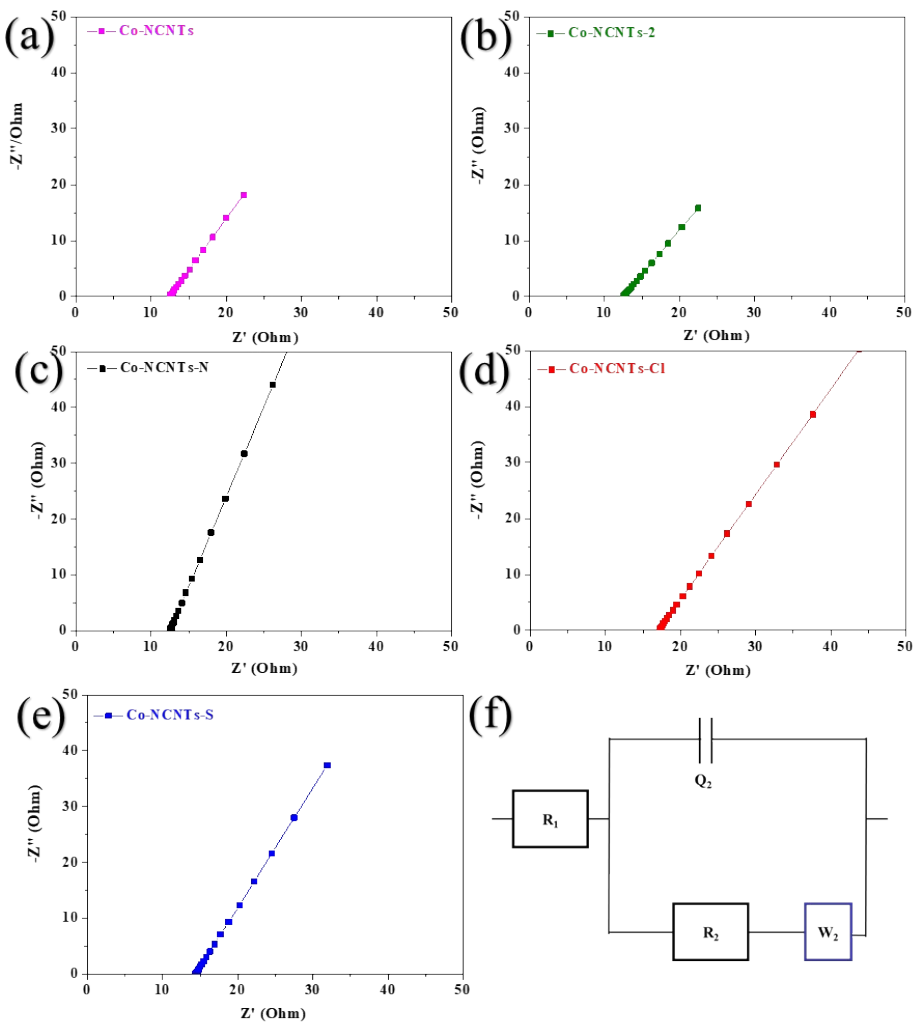


Figure S14. EIS of (a) Co-NCNTs, (b) Co-NCNTs-2, (c) Co-NCNTs-N, (d) Co-NCNTs-Cl and (e) Co-NCNTs-S. (f) Fitted circuit.

Table S1. Contact resistance (R_1) and diffusion resistance (R_2) calculated by fitted circuit for each samples.

Sample	R_1 (Contact resistance)	R_2 (Diffusion resistance)
Co-NCNTs	12.52 Ohm	2.847×10^{12} Ohm
Co-NCNTs-2	12.53 Ohm	5.843×10^{12} Ohm
Co-NCNTs-N	12.44 Ohm	1.952×10^{11} Ohm
Co-NCNTs-Cl	17.07 Ohm	4.437×10^{15} Ohm
Co-NCNTs-S	14.39 Ohm	1.538×10^{14} Ohm

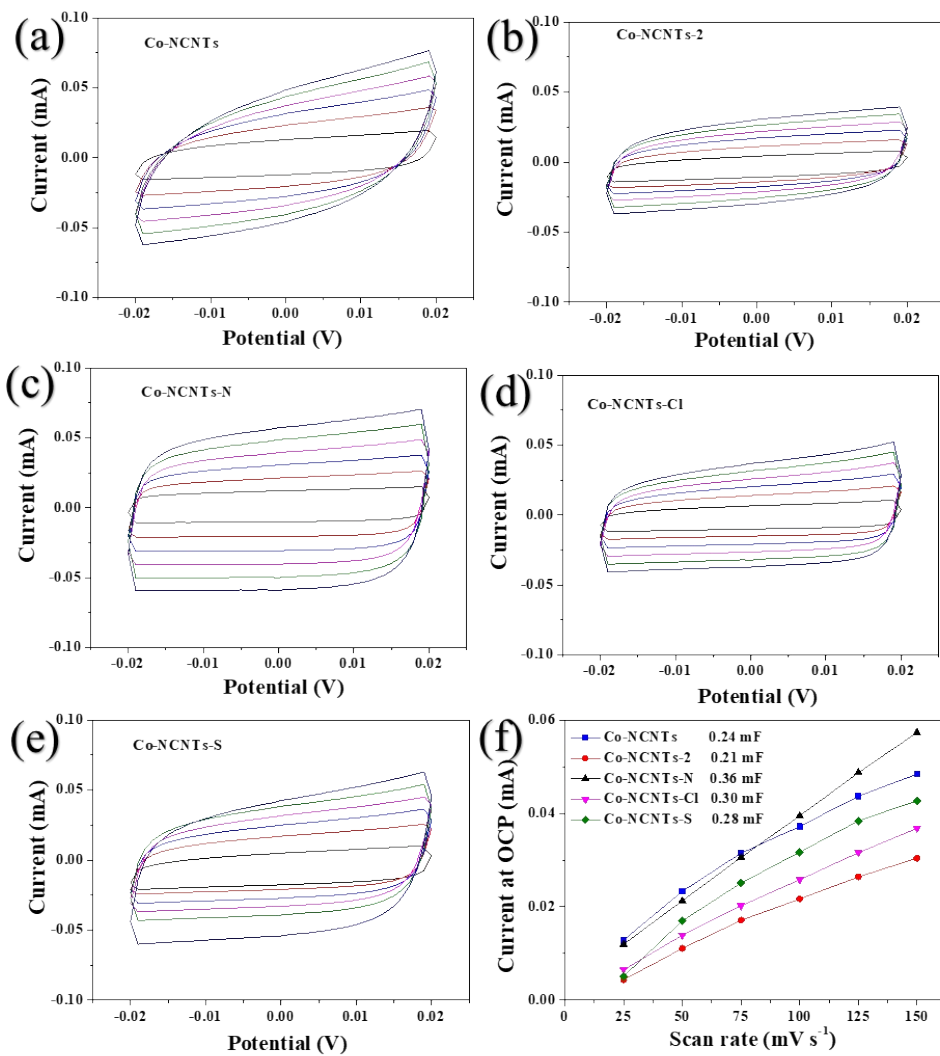


Figure S15. Cyclic voltammograms (CVs) tested at the potential range from 0.02 to 0.02 V vs. open circuit potential (OCP) with the scan rates increasing from 25 to 150 mV s^{-1} for (a) Co-NCNTs, (b) Co-NCNTs-2, (c) Co-NCNTs-N, (d) Co-NCNTs-Cl and (e) Co-NCNTs-S. (f) Plots of the current at OCP vs. the scan rate of Co-NCNTs, Co-NCNTs-2, Co-NCNTs-N, Co-NCNTs-Cl and Co-NCNTs-S.

Table S2. Comparison of Co-NCNT-N with Co-based electrocatalysts for ZABs.

Catalyst	ORR half-wave potential ($E_{1/2}$) (V vs. RHE)	OER potential at 10 mA cm ⁻² (V vs. RHE)	Power density (mW cm ⁻²)	Ref.
Co-NCNT-N	0.80 V	1.58 V	210	This Work
CoN ₄ /NG	0.87 V	1.61	115	1
Co/Co ₃ O ₄ @PGS	0.89 V	1.58 V	118	2
Co@NCNTA-700	0.86 V	1.51 V	38	3
Co/Co ₉ S ₈ @CNTs-900	0.92 V	1.64 V	184	4
Co-SAs@NC	0.82 V	—	105	5
Co-N-C SAC	0.85 V	1.67 V	143	6
Co-NCNT/Ng-900	0.81 V	—	174	7
Co-SAs/SNPs@NC	0.89 V	—	223	8
CoSx/Co-NC-800	0.80 V	1.54 V	103	9
CCO@C	0.86 V	1.55 V	—	10
CoP NCs	0.85 V	1.56 V	62	11
NC-Co SA	0.87 V	1.58 V	20	12
A-Co@CMK-3-D-	0.83 V	—	162	13
CoSA@NCF/CNF	0.88 V	1.68 V	—	14
CoSAs/N-CNS	0.91 V	—	157	15
Co _p @CoNC	0.84	1.52 V	188	16

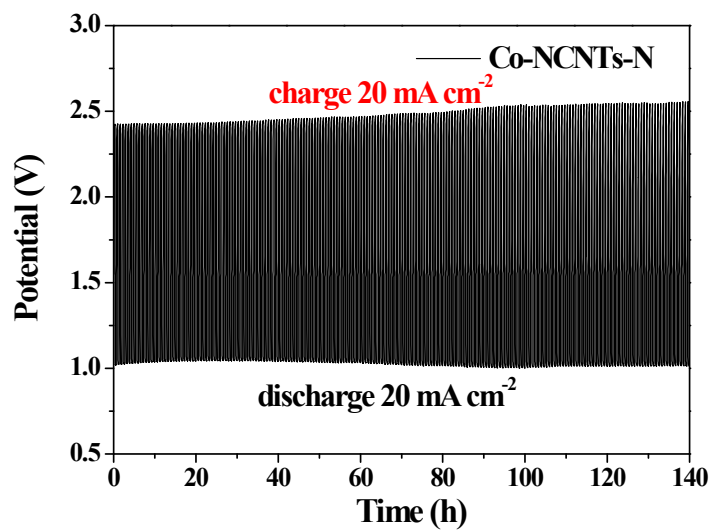


Figure S16. Charge-discharge cycling performance of Co-NCNTs-N based oxygen electrode for Zn-air batteries at 20 mA cm^{-2} .

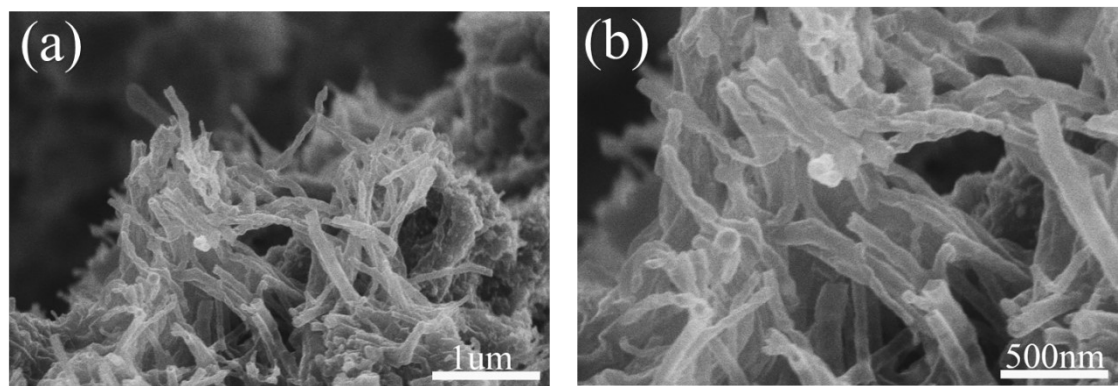


Figure S17. SEM images of Co-NCNTs-N after 130 h charge-discharge cycling tests for Zn-air batteries.

References

- 1 L. Yang, L. Shi, D. Wang, Y. Lv and D. Cao, Single-atom cobalt electrocatalysts for foldable solid-state Zn-air battery, *Nano Energy*, 2018, **50**, 691-698.
- 2 Y. Jiang, Y.-P. Deng, J. Fu, D. U. Lee, R. Liang, Z. P. Cano, Y. Liu, Z. Bai, S. Hwang, L. Yang, D. Su, W. Chu and Z. Chen, Interpenetrating Triphase Cobalt-Based Nanocomposites as Efficient Bifunctional Oxygen Electrocatalysts for Long-Lasting Rechargeable Zn-Air Batteries, *Adv. Energy Mater.*, 2018, **8**, 1702900.
- 3 L. Liu, Y. Wang, F. Yan, C. Zhu, B. Geng, Y. Chen and S. I. Chou, Cobalt-Encapsulated Nitrogen-Doped Carbon Nanotube Arrays for Flexible Zinc–Air Batteries, *Small Methods*, 2019, **4**, 1900571.
- 4 H.-M. Zhang, C. Hu, M. Ji, M. Wang, J. Yu, H. Liu, C. Zhu and J. Xu, Co/Co₉S₈@carbon nanotubes on a carbon sheet: facile controlled synthesis, and application to electrocatalysis in oxygen reduction/oxygen evolution reactions, and to a rechargeable Zn-air battery, *Inorg. Chem. Front.*, 2021, **8**, 368-375.
- 5 X. Han, X. Ling, Y. Wang, T. Ma, C. Zhong, W. Hu and Y. Deng, Generation of Nanoparticle, Atomic-Cluster, and Single-Atom Cobalt Catalysts from Zeolitic Imidazole Frameworks by Spatial Isolation and Their Use in Zinc-Air Batteries, *Angew. Chem. Int. Ed.*, 2019, **58**, 5359-5364.
- 6 L. Wang, Z. Xu, T. Peng, M. Liu, L. Zhang and J. Zhang, Bifunctional Single-Atom Cobalt Electrocatalysts with Dense Active Sites Prepared via a Silica Xerogel Strategy for Rechargeable Zinc-Air Batteries, *Nanomaterials*, 2022, **12**, 381.
- 7 K. Fu, Y. Wang, L. Mao, X. Yang, J. Jin, S. Yang and G. Li, Strongly coupled Co, N co-doped carbon nanotubes/graphene-like carbon nanosheets as efficient oxygen reduction electrocatalysts for primary Zinc-air battery, *Chem. Eng. J.*, 2018, **351**, 94-102.
- 8 Z. Wang, C. Zhu, H. Tan, J. Liu, L. Xu, Y. Zhang, Y. Liu, X. Zou, Z. Liu and X. Lu, Understanding the Synergistic Effects of Cobalt Single Atoms and Small Nanoparticles: Enhancing Oxygen Reduction Reaction Catalytic Activity and Stability for Zinc-Air Batteries, *Adv. Funct. Mater.*, 2021, **31**, 2104735.
- 9 Q. Lu, J. Yu, X. Zou, K. Liao, P. Tan, W. Zhou, M. Ni and Z. Shao, Self-Catalyzed Growth of Co, N-Codoped CNTs on Carbon-Encased CoS_x Surface: A Noble-Metal-Free Bifunctional Oxygen Electrocatalyst for Flexible Solid Zn–Air Batteries, *Adv. Funct. Mater.*, 2019, **29**, 1904481.
- 10 X. Wang, Y. Li, T. Jin, J. Meng, L. Jiao, M. Zhu and J. Chen, Electrospun Thin-Walled CuCo₂O₄@C Nanotubes as Bifunctional Oxygen Electrocatalysts for Rechargeable Zn-Air Batteries, *Nano Lett.*, 2017, **17**, 7989-7994.
- 11 H. Li, Q. Li, P. Wen, T. B. Williams, S. Adhikari, C. Dun, C. Lu, D. Itanze, L. Jiang, D. L. Carroll, G. L. Donati, P. M. Lundin, Y. Qiu and S. M. Geyer, Colloidal Cobalt Phosphide Nanocrystals as Trifunctional Electrocatalysts for Overall Water Splitting Powered by a Zinc-Air Battery, *Adv. Mater.*, 2018, **30**, 1705796.
- 12 W. Zang, A. Sumboja, Y. Ma, H. Zhang, Y. Wu, S. Wu, H. Wu, Z. Liu, C. Guan, J. Wang and S. J. Pennycook, Single Co Atoms Anchored in Porous N-Doped Carbon for Efficient Zinc–Air Battery Cathodes, *ACS Catal.*, 2018, **8**, 8961-8969.
- 13 X. Lyu, G. Li, X. Chen, B. Shi, J. Liu, L. Zhuang and Y. Jia, Atomic Cobalt on Defective Bimodal Mesoporous Carbon toward Efficient Oxygen Reduction for Zinc–Air Batteries, *Small Methods*, 2019, **3**, 1800450.
- 14 D. Ji, L. Fan, L. Li, S. Peng, D. Yu, J. Song, S. Ramakrishna and S. Guo, Atomically Transition

- Metals on Self-Supported Porous Carbon Flake Arrays as Binder-Free Air Cathode for Wearable Zinc-Air Batteries, *Adv. Mater.*, 2019, **31**, e1808267.
- 15 D. Wang, M. Yuan, J. Xu, Y. Li, K. Shi, H. Yang, H. Li and G. Sun, Highly Active Atomically Dispersed Co-N_x Sites Anchored on Ultrathin N-Doped Carbon Nanosheets with Durability Oxygen Reduction Reaction of Zinc–Air Batteries, *ACS Sustain. Chem. Eng.*, 2021, **9**, 16956-16964.
- 16 H. Yang, S. Gao, D. Rao and X. Yan, Designing superior bifunctional electrocatalyst with high-purity pyrrole-type CoN₄ and adjacent metallic cobalt sites for rechargeable Zn-air batteries, *Energy Storage Mater.*, 2022, **46**, 553-562.